

Modelling and simulation of a power converter for variable speed hydrokinetic systems

P.B. Ngancha, K. Kusakana*, E. Markus

Abstract— This study presents the control scheme model of a micro-hydrokinetic turbine system equipped with a permanent magnet synchronous generator (PMSG). A power conversion system model is developed to allow a variable speed hydrokinetic turbine system to generate constant voltage and frequency at variable water speeds. A DC-DC boosting chopper is used to maintain constant DC link voltage. The DC current is regulated to follow the optimized reference current for maximum power point tracking (MPPT) operation of the turbine system. The DC link voltage is controlled to feed the current into the load through the line-side pulse width modulation (PWM) inverter. The proposed scheme is modelled and simulated using MATLAB/Simulink. The results show a high quality power conversion solution for a variable speed hydrokinetic river system.

Index Terms— Hydrokinetic, AC-DC-AC power converter, modelling, performance analysis

1 INTRODUCTION

Rapid economic development and population growth has led to severe environmental pollution due to energy demand growth. Making use of the available renewable energy sources can optimally mitigate global warming through the reduction of greenhouse gases (GHGs) [1]. There is a huge demand for affordable electrical energy, particularly for low-income inhabitants in Africa [2]. Electricity shortage due to lack of research leads to blackouts that may result into economic losses [3]. The exploration of the available renewable energy sources can bring about an affordable electrification means, especially for poor remote rural residents. The main challenge with renewable energy is the intermittent nature of renewable energy sources due to variable climatic conditions (e.g. water flow rate, solar intensity, wind speed, etc.). The variation of renewable energy sources leads to the variation of the generated output voltage and frequency [4]. Power electronics devices with variable speed control capabilities are very important.

Hydrokinetic systems are among promising renewable energy power generation methods that generate electricity through the use of an underwater wind turbine to extract the kinetic energy of flowing water instead of the potential energy of falling water [5-9]. This is a financially viable solution for poor rural residents since it does not require the construction of civil structures (dams, weirs, channels, etc.). However, the variable water speed may cause the

hydrokinetic turbine to rotate at variable speeds and still allow the permanent magnet synchronous generator (PMSG) to generate variable voltage with variable frequencies. The alternating voltage with variable frequency is not suitable for used by the load or public electrical grid. Hence, it is important to control the generated output voltage of the hydrokinetic system in terms of amplitude and frequency during fluctuating water flow.

This paper presents a control strategy of a hydrokinetic turbine driven PMSG in order to maintain constant voltage amplitude and frequency at variable water speeds. The reason for selecting a PMSG over other types of generators is its ability to operate at low speed and also to improve the reliability of the variable speed hydrokinetic system. Low speed operation capability eliminates the requirement for a gearbox which often suffers from mechanical faults and thus reduces the efficiency of the overall system. Therefore, a direct driven PMSG has been selected in this study. A maximum power point tracking (MPPT) has been used to extract maximum power from the flowing water since it varies with change in water speed. A sensorless maximum power extraction method has been used. The sensorless MPPT technique is used because the ones that use mechanical speed sensors are inaccurate. They require sensors with tolerable accuracy to track the maximum output power of the hydrokinetic turbine system.

The pulse width modulator (PWM) converter, DC-DC booster and inverter have been used to model the proposed control approach. The controlled DC-DC boosting converter has been used to control the output power of a hydrokinetic system by sensing the rectified voltage and tracing the maximum power point. Hence, the DC link voltage is kept constant under variable water speeds. The inverter at the load side is used to supply constant output voltage in terms of amplitude and frequency. Both the active and reactive power of the stator windings are regulated through control of dq-axis rotor currents. The q-axis current regulates the active power and while the d-axis regulates the reactive power. The validation of the model is fulfilled through simulation carried out using MATLAB/Simulink program. The simulation results proved that the control strategy works very well for the proposed hydrokinetic turbine system under variable flowing water speeds.

B.P. Ngancha, Central University of Technology, Private Bag X20539, Bloemfontein 9300, South Africa (e-mail: padbonn@yahoo.com).

K. Kusakana, Central University of Technology, Private Bag X20539, Bloemfontein 9300, South Africa (e-mail: kkusakana@cut.ac.za).

E.D. Markus, Central University of Technology, Private Bag X20539, Bloemfontein 9300, South Africa (e-mail: emarkus@cut.ac.za).

2 MICRO-HYDROKINETIC CONTROL SYSTEM OVERVIEW

The layout of the modelled micro-hydrokinetic river control (MHRC) system consists of a turbine, mechanical drive-train, PMSG, and a control system. The turbine is connected to the generator via the mechanical drive-train through the rotor shaft. The hydrokinetic turbine converts the kinetic energy of flowing water into mechanical energy so as to drive the PMSG via the shaft. The mechanical drive ratio is considered to be 1:1 since no gearbox has been used. The power electronic control (PEC) system is connected to the output of the PMSG to supply AC voltage having constant amplitude and frequency to a three phase balanced load. The generated electrical energy is fed into the PEC system to stabilise the variable voltage into a constant amplitude and frequency source before supplying the load.

2.1 Hydrokinetic turbine model

The mechanical power extracted by a hydrokinetic turbine is less than the power of the moving water. Only a fraction of the total kinetic power can be extracted due to losses. Hence, the power coefficient is limited to 59.3% as tested by the well-known Betz law. The mechanical power extracted by a hydrokinetic turbine is expressed as follows [10]:

$$P_m = \frac{1}{2} \rho A v^3 C_p \quad (1)$$

Where: ρ is the water density (1000kg/m³), A is the swept area of the turbine rotor blades (m²), v is the flowing water velocity and C_p is turbine power coefficient.

The turbine power coefficient (C_p) relies on the tip-speed ratio (λ) and the blade pitch angle (β) and can be expressed using the empirical coefficient of a typical hydrokinetic system as shown in Eq. 2 [8]:

$$C_p(\lambda, \beta) = 0.5176 \left(116 \frac{1}{\lambda_i} - 0.4\beta - 5 \right) e^{\left(\frac{-21}{\lambda_i} \right)} + 0.0068\lambda \quad (2)$$

The parameter λ_i is determined using the following equation:

$$\lambda_i = 1 / \left(\frac{1}{\lambda + 0.08\beta} - \frac{0.035}{1 + \beta^3} \right) \quad (3)$$

A direct drive one-mass drive-train model has been used between the turbine and the PMSG.

2.2 Permanent magnet synchronous generator (PMSG) model

When modelling a PMSG, the d-q synchronous reference frame components are used to derive the model. The d-axis components and q-axis components can be controlled to influence the active and reactive power, respectively. By assuming that the flow direction of the negative stator current is out of the generator positive polarity terminals, the d-q reference stator voltages can be expressed as follows [9]:

$$v_d = R_s i_d + L_d \frac{di_d}{dt} - \omega_e L_q i_q \quad (4)$$

$$v_q = R_s i_q + L_q \frac{di_q}{dt} - \omega_e \psi_{pm} + \omega_e L_d i_d \quad (5)$$

Where: v_d and v_q are the stator terminal voltages in the d-q axis reference frame (V), R_s is the stator resistance (Ω), L_d and L_q are the d, q axis reference frame inductances (H), i_d and i_q are the d, q axis reference frame stator currents (A), and ω_e is the electrical angular speed (rad/sec).

Equations (4) and (5) can be rearranged to obtain the output d and q currents of the generator as follows:

$$i_d = \int \left(\frac{v_d}{L_d} - \frac{R_s}{L_d} i_d + \frac{L_q}{L_d} \omega_e i_q \right) \quad (6)$$

$$i_q = \int \left(\frac{v_q}{L_q} - \frac{R_s}{L_q} i_q + \frac{L_d}{L_q} \omega_e i_d - \frac{\psi_{pm}}{L_q} \omega_e \right) \quad (7)$$

In the d-q synchronous rotating reference frame, the electromagnetic torque (T_e) is presented as follows:

$$T_e = \frac{3}{2} (\psi_{pm} \cdot i_q + (L_d - L_q) i_d \cdot i_q) \quad (8)$$

Where: p is the number of pole pairs.

The transformation of the three phase alternating current or voltage quantities into direct current or voltage (d-q) quantities is made possible by means of Park's Transformation method, as shown in Equation (11) [10]. This method transforms the parameters and equation from the stationary form into direct-quadrature (d-q) axis. For a salient pole permanent magnet synchronous machine, d and q axis inductances are almost equal due to a large and constant air gap. The dynamic model of a permanent magnet synchronous machine is derived from a two-phase synchronous reference frame, in which the q-axis is 90° ahead of the d-axis with respect to the direction of rotation.

The relationship between the electrical angular speed (ω_e) and rotor angular speed of the generator (ω_g) is expressed as follows:

$$\omega_e = p \cdot \omega_g \quad (9)$$

The relationship between ω_e and electrical angle (θ_e) is expressed as follows:

$$\frac{d\theta_e}{dt} = \omega_e \quad (10)$$

The conversion of three-phase voltage variables into DC voltage variables is done as follows:

$$\begin{pmatrix} v_d \\ v_q \\ v_0 \end{pmatrix} \frac{2}{3} \begin{pmatrix} \cos \theta_e & \cos(\theta_e - \frac{2\pi}{3}) & \cos(\theta_e + \frac{2\pi}{3}) \\ \sin \theta_e & \sin(\theta_e - \frac{2\pi}{3}) & \sin(\theta_e + \frac{2\pi}{3}) \\ \frac{1}{2} & \frac{1}{2} & \frac{1}{2} \end{pmatrix} \begin{pmatrix} V_a \\ V_b \\ V_c \end{pmatrix} \quad (11)$$

To simplify the model, the zero phase sequence component can be ignored and equation (11) then becomes:

$$\begin{pmatrix} v_d \\ v_q \end{pmatrix} \frac{2}{3} \begin{pmatrix} \cos \theta_e & \cos(\theta_e - \frac{2\pi}{3}) & \cos(\theta_e + \frac{2\pi}{3}) \\ \sin \theta_e & \sin(\theta_e - \frac{2\pi}{3}) & \sin(\theta_e + \frac{2\pi}{3}) \end{pmatrix} \begin{pmatrix} V_a \\ V_b \\ V_c \end{pmatrix} \quad (12)$$

2.3 Feedback I_{dq} controller model

Since the hydrokinetic power fluctuates with water speed, the PMSG output voltage and frequency vary continuously. The controller plays an important role in solving this problem. The I_{dq} current controller is responsible for affecting the reference current magnitude and angle within the stator. The design of the current controller is based on the v_d and v_q voltages.

Let:

$$v_d(t) = \frac{V_{dc}}{2} m_d(t) \quad (13)$$

$$v_q(t) = \frac{V_{dc}}{2} m_q(t) \quad (14)$$

Where: m_d and m_q represents the direct and quadrature axis modulation signals.

Due to the presence of $L\omega_0$ terms in Equation (15) and (16), the dynamics of i_d and i_q are coupled. To decouple these dynamics, we determine m_d and m_q as:

$$m_d(t) = \frac{2}{V_{dc}} (v_d - L\omega_0 i_q) \quad (15)$$

$$m_q(t) = \frac{2}{V_{dc}} (v_q - L\omega_0 i_d) \quad (16)$$

Where: L is the inductance, ω_0 is the angular frequency.

The d-axis gain is given by:

$$k_d(s) = \frac{(K_p s + k_i)}{s} \quad (17)$$

Where K_p and k_i are proportional and integral gains, respectively. Thus, the loop gain is expressed as:

$$I(s) = \left(\frac{k_p}{L_s} \right) \frac{s + k_i/k_p}{s + (R + r_{on})/L} \quad (18)$$

It is noted that due to the plant pole at $s = -(R + r_{on})/L$, which is fairly close to the origin, the magnitude and the phase of the loop gain start to drop from a relatively low frequency. Thus, the plant pole is first cancelled by the compensator zero, $s = -\frac{k_i}{k_p}$ and the loop gain assumes the form, $E(s) = \frac{k_p}{L_s}$. Then, the closed-loop transfer function, $E(s)/(1 + E(s))$, becomes:

$$\frac{I_d(s)}{I_{dref}(s)} = G_i(s) = \frac{1}{\tau_i s + 1} \quad (19)$$

With,

$$k_p = L/\tau_i \quad (20)$$

$$k_i = (R + r_{on})/\tau_i \quad (21)$$

Where τ_i is the time constant of the resultant closed-loop system.

Equation (19) indicates that, if k_p and k_i are selected based on (20) and (21), the response of $i_d(t)$ to $i_{dref}(t)$ is based on a first-order transfer function, whose time constant τ_i is a design choice. τ_i Should be made small for a fast current-control response but adequately large so that $1/\tau_i$, that is, the bandwidth of the closed-loop control system, is considerably smaller. For example, it can be made 10 times smaller than the switching frequency of the DC-DC controller (expressed in rad/s). Depending on the requirements of a specific application and the converter switching frequency, τ_i is typically selected in the range of 0.5-5 ms. The same compensator as $k_d(s)$ is also adopted for the q-axis compensator $k_q(s)$ as in the d-q model.

Based on (22) and (23), i_d and i_q can be controlled by v_d and v_q , respectively. The d-axis compensator processes $e_d = i_{dref} - i_d$ provides a v_d voltage.

$$L \frac{di_d}{dt} = V_d - (R + r_{on})i_d \quad (22)$$

$$L \frac{di_q}{dt} = V_q - (R + r_{on})i_q \quad (23)$$

Where: r_{on} is the resistance due to mutual induction.

Then, based on Equation (15), it can be seen that v_d contributes to m_d . Similarly, the q-axis compensator processes $e_q = i_{qref} - i_q$ and provides v_q voltage that contributes to m_q . The controller then amplifies m_d and m_q by a factor of $V_{dc}/2$ and generates V_d and V_q that, in turn, control i_d and i_q based on (6) and (7).

To make i_d and i_q the subject of the formula, Equation (22) and (23) can be rearranged as follows:

$$i_d = \int \left(\frac{v_d}{L} - \frac{(R + r_{on})}{L} i_d \right) \quad (24)$$

$$i_q = \int \left(\frac{v_q}{L} - \frac{(R + r_{on})}{L} i_q \right) \quad (25)$$

The conversion of i_{dq0} back to i_{abc} after the control block is made possible by means of reverse Park's transformation, as shown in equation (26) below:

$$\begin{pmatrix} i_d \\ i_q \\ i_c \end{pmatrix} = \frac{2}{3} \begin{pmatrix} \cos \theta_e & \sin \theta_e & 1 \\ \cos(\theta_e - \frac{2\pi}{3}) & \sin(\theta_e - \frac{2\pi}{3}) & 1 \\ \cos(\theta_e + \frac{2\pi}{3}) & \sin(\theta_e + \frac{2\pi}{3}) & 1 \end{pmatrix} \begin{pmatrix} i_d \\ i_q \\ i_0 \end{pmatrix} \quad (26)$$

When zero phase sequence component is ignored, equation (27) becomes:

$$\begin{pmatrix} i_d \\ i_q \\ i_c \end{pmatrix} = \frac{2}{3} \begin{pmatrix} \cos \theta_e & \sin \theta_e & 1 \\ \cos(\theta_e - \frac{2\pi}{3}) & \sin(\theta_e - \frac{2\pi}{3}) & 1 \\ \cos(\theta_e + \frac{2\pi}{3}) & \sin(\theta_e + \frac{2\pi}{3}) & 1 \end{pmatrix} \begin{pmatrix} i_d \\ i_q \end{pmatrix} \quad (27)$$

Finally, the three phase output currents (i_{abc}) in equations (28), (29) and (30) are then used to supply a three phase load,

or can be injected into an electrical power grid system for utilization.

$$\frac{di_a}{dt} = \frac{1}{L}(v_a(t) + i_a R_s + v_a) \quad (28)$$

$$\frac{di_b}{dt} = \frac{1}{L}(v_b(t) + i_b R_s + v_b) \quad (29)$$

$$\frac{di_c}{dt} = \frac{1}{L}(v_c(t) + i_c R_s + v_c) \quad (30)$$

2.4 Final Simulink block diagram of the developed converter

Figure 1 shows the overall MHRC system Simulink block diagram for the complete processes from the turbine, drive-train, generator, control and to the three-phase load. The main objective is to use the overall Simulink model to test the proposed control system performance under variable water flow speed.

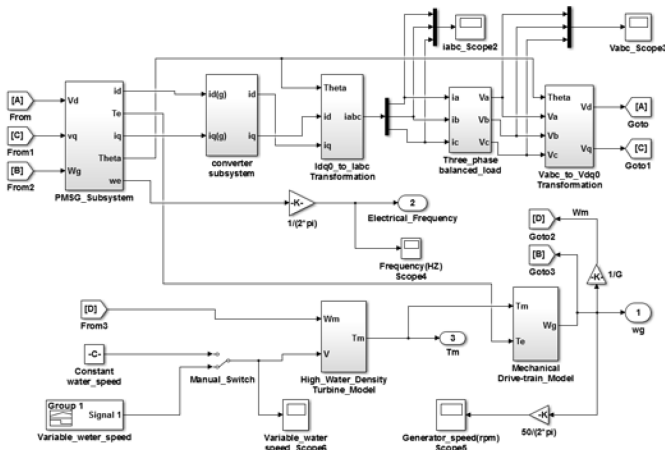


Figure 1: Simulink block diagram of an overall MHRC system model

3 RESULTS AND DISCUSSION

Two different cases were investigated in order to reveal the quality of the proposed power conversion solution for the variable speed hydrokinetic river system. The first case shows the simulation results of the variable speed hydrokinetic river system without the inclusion of the converter (controller). The second case will reveal the simulation results with the inclusion of the converter in the variable speed hydrokinetic river system.

Table I: PMSG parameters [10-11].

Categories	Values
Stator phase resistance	2
Number of pole pairs	8
d-q axis inductance	1 mH
Permanent magnet flux	0.46 Wb
Rated rotor speed	375 rpm
Rated power	2 kW
Rated phase voltage	120 V
Rated phase current	17 A
Rated frequency	50 Hz
Balance three phase load	20kw

The selected PMSG is capable of generating 132.37 V, 50 Hz at a rated full load speed of 377.2rpm, as shown in Table 1. During the simulations, it has been assumed that the water flow velocity varies from 0.45 to 2.58 m/s.

3.1 Case 1: micro-hydrokinetic river system performance without AC-DC-AC converter.

This section shows the simulation results based on the performance of a micro-hydrokinetic turbine system equipped with a permanent magnet synchronous generator (PMSG) under variable water speed and without the converter (control) system.

Based on the operation principle of synchronous generators, the rotational speed of the generator together with the number of poles determines the frequency of the induced voltage. From Figure 2 and Figure 3, it can be noticed that at any point in time, the angular speed of the generator changes directly in proportion to the change in water flow speed. When the speed of the water increases to 2.58 m/s (from $t = 4$ s to 5 s), the generated voltage reaches 187.2 V-peak as observe in figure 4 and at a frequency close to 50 Hz refer in figure 6. The variations of the water flow speed also relate to the variation of the generated voltage, current and frequency magnitude, as seen in figures 4, 5 and 6 respectively.

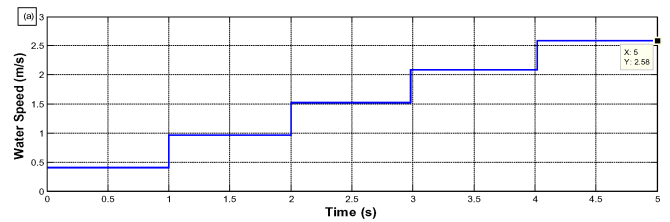


Figure 2: Water speed

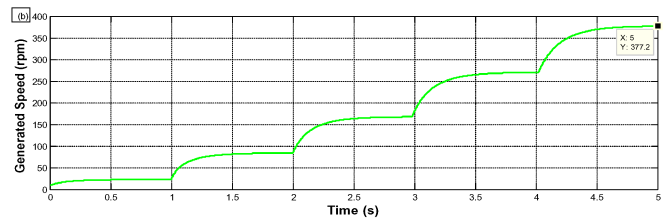


Figure 3: Generator speed

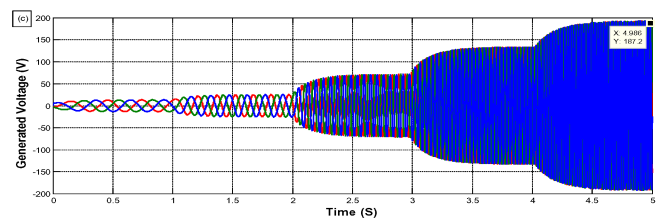


Figure 4: Generated Voltage

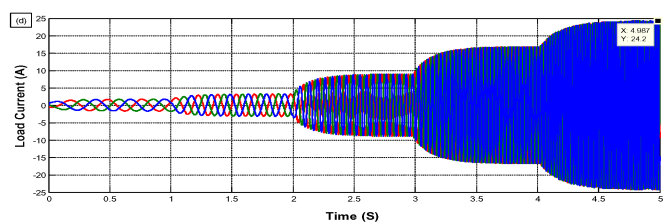


Figure 5: Load Current

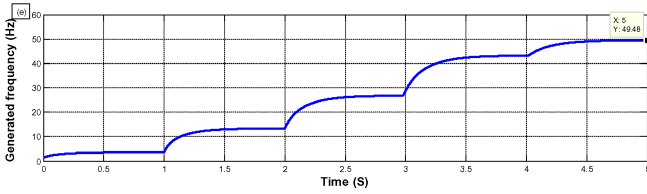


Figure 6: Electrical frequency

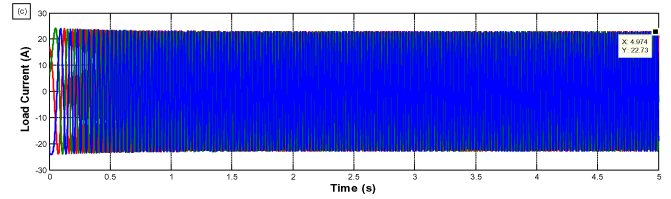


Figure 10: Load Current (with converter)

3.2 Case 2: micro-hydrokinetic river system performance with the inclusion of AC-DC-AC converter.

This section shows the simulation results based on the performance of a micro-hydrokinetic turbine system under variable water speed and with the inclusion of the converter (control) system. The converter is a build electronic circuit that transform different voltage magnitude to a constant voltage level.

As explained in section 2, the converter in this case is used to transform the variable AC input I_{acb} into a DC I_{dq0} by using equation 11 and 12. The DC to DC current-mode control pulse-width modulation controller (PWM) is adopted resulting in the variation of the average value of the waveform. Figure 7 shows that; between $t=0s$ to $t=2s$, a growth in frequency due to the weak input signal, at the time when its approaches $t=2s$ to $t=5s$, the frequency riches 50Hz, finally the DC I_{dq0} signal is transformed back to I_{acb} quantity with the help of equation 26 and 27.

Figure 8 shows that, with the inclusion of the converter into the system, a constant voltage level is obtained at the output of the converter to a value of 182.8V-peak to supply the load, while Figure 9 gives a clearer view of the results displayed in Figure 8 for the time period between 3s and 3.1s.

Figure 10 shows that, the converter output current of 22.86A-peak is witness across the load. Figure 11 gives a clearer view of Figure 10 taken for a time period between 3 and 3.1second.

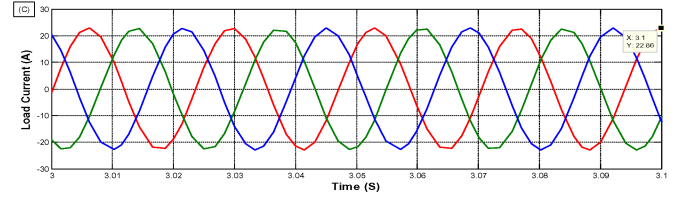


Figure 11: Load Current (extended)

4 CONCLUSION

This paper presented the modelling and control technique of a variable-speed hydrokinetic turbine system comprised a PMSG. The main aim of the investigation was to make use of the power electronic control system to prevent voltage deviation in a hydrokinetic turbine system due to variable flowing water speed constraints. The proposed AC-DC-AC control model has been developed using the MATLAB/Simulink program. Through the inclusion of the converter between the generator and the load, the constant voltage in terms of the amplitude and frequency was achieved at variable water flow speeds. This was made possible through maintenance of a constant control reference setting. Hence, the proposed control algorithm is suitable for the hydrokinetic turbine generation system as revealed by the simulation results. This presents a necessity for future implementation of hydrokinetic generation systems to supply electricity to isolated rural loads or to sell energy to the grid.

REFERENCES

- [1] Goedeckeb M, Therdthianwong S, Gheewala SH. "Life cycle cost analysis of alternative vehicles and fuels in Thailand". *Energy Policy* 35:6 (2007) 3236-46.
- [2] Kusakana K., Vermaak H.J. "Hybrid renewable power systems for mobile telephony base station in developing countries". *Elsevier Renewable Energy* 51 (2013) 419-425.
- [3] Hachimenum N. A. "Impact of Power Outages on Developing Countries: Evidence from Rural Households in Niger Delta, Nigeria". *Journal of Energy Technologies and Policy*, 5:3 (2015) 2225-0573.
- [4] Hussein M.M., Senjyu T., Orabi M., Wahab M.A.A., Hamada M.M. "Control of a Stand-alone Variable Speed Wind Energy Supply System". *Applied Science* 3 (2013) 437-456.
- [5] Kusakana K. "Energy management of a grid-connected hydrokinetic system under Time of Use tariff". *Renewable Energy* 101 (2017) 1325-1333.
- [6] Kusakana K., Vermaak H.J. "Hydrokinetic power generation for rural electricity supply: Case of South Africa". *Renewable Energy* 55 (2013) 467-473.
- [7] Kusakana K., Vermaak H.J. "Cost and performance evaluation of hydrokinetic-diesel hybrid systems". *Energy Procedia* 61 (2014), 2439-2442.
- [8] Kusakana K. "Optimisation of the daily operation of a Hydrokinetic-Diesel generator power plant". *International Conference on the Industrial and Commercial Use of Energy (ICUE 2014)*. Cape Town, South Africa, pp. 367-372.
- [9] Kusakana K. "Optimal operation scheduling of a Hydrokinetic-Diesel hybrid system with Pumped Hydro Storage". *4th International Conference on Electric Power and Energy Conversion Systems (EPECS 2015)*. Sharjah, UAE, pp. 1-6.

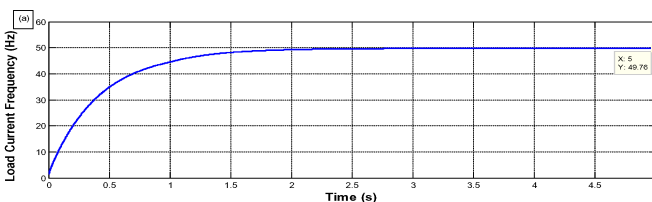


Figure 7: Electrical frequency (with converter)

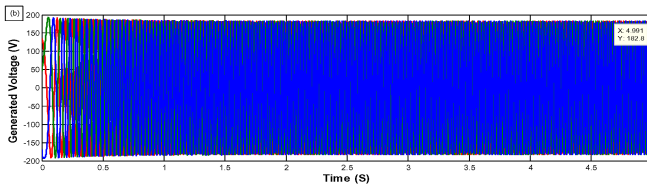


Figure 8: Load Voltage (with converter)

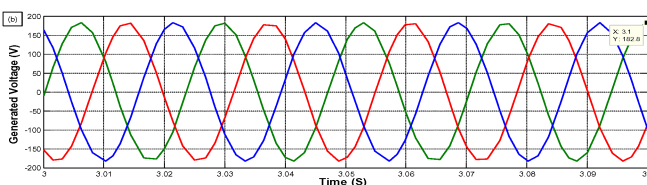


Figure 9: Load Voltage (extended)

- [10] Koko S.P., Kusakana K., Vermaak H.J. "Micro-hydrokinetic River system modelling and analysis as compared to wind system for remote rural electrification". *Electric Power Systems Research* 126 (2015) 38-44.
- [11] Koko S.P., Kusakana K., Vermaak H.J. "Modelling and performance analysis of a micro-hydrokinetic river system as compared to wind system". *South African University Power and Energy conference (SAUPEC 2015)*. Johannesburg, South Africa, pp. 141-147.

AUTHORS BIOS AND PHOTOGRAPHS



P.B. Ngancha holds B. Tech in Electrical Engineering. He is currently busy with M.Eng. studies in Electrical Engineering at the Central University of Technology. His current research focus is on modelling and simulation of power converters for variable speed hydrokinetic system, renewable and sustainable energy systems.



K. Kusakana holds a D. Tech in Electrical Engineering. He is currently a senior lecturer, researcher and Head of the Electrical, Electronic and Computer Engineering Department at the Central University of Technology. His research interests are energy management, renewable and alternative energies.



ED Markus holds an M. Eng degree in Electrical Engineering. He is currently a lecturer in the Electrical Engineering Department at the Central University of Technology. His research interests are nonlinear control, robotics, Power systems, Differential Flatness, Telecommunications and artificial intelligence.

This paper will be presented by P.B. Ngancha